Tumor endothelial marker 1–specific DNA vaccination targets tumor vasculature

John G. Facciponte,[1] Stefano Ugel,[1] Francesco De Sanctis,[1,2] Chunsheng Li,[1] Liping Wang,[3] Gautham Nair,[4] Sandy Sehgal,[5] Arjun Raj,[4] Efthymia Matthaiou,[1] George Coukos,[1] and Andrea Facciabene[1]

[1]Ovarian Cancer Research Center (OCRC), University of Pennsylvania School of Medicine, Philadelphia, Pennsylvania, USA. [2]Department of Experimental Medicine and Biochemical Science, University of Perugia, Perugia, Italy. [3]Department of Pathology and Laboratory Medicine, [4]Department of Bioengineering, and [5]Department of Radiology, University of Pennsylvania, Philadelphia, Pennsylvania, USA.

Tumor endothelial marker 1 (TEM1; also known as endosialin or CD248) is a protein found on tumor vasculature and in tumor stroma. Here, we tested whether TEM1 has potential as a therapeutic target for cancer immunotherapy by immunizing immunocompetent mice with *Tem1* cDNA fused to the minimal domain of the C fragment of tetanus toxoid (referred to herein as Tem1-TT vaccine). Tem1-TT vaccination elicited $CD8^+$ and/or $CD4^+$ T cell responses against immunodominant TEM1 protein sequences. Prophylactic immunization of animals with Tem1-TT prevented or delayed tumor formation in several murine tumor models. Therapeutic vaccination of tumor-bearing mice reduced tumor vascularity, increased infiltration of $CD3^+$ T cells into the tumor, and controlled progression of established tumors. Tem1-TT vaccination also elicited $CD8^+$ cytotoxic T cell responses against murine tumor-specific antigens. Effective Tem1-TT vaccination did not affect angiogenesis-dependent physiological processes, including wound healing and reproduction. Based on these data and the widespread expression of TEM1 on the vasculature of different tumor types, we conclude that targeting TEM1 has therapeutic potential in cancer immunotherapy.

Introduction

Angiogenesis, the growth of new blood vessels from preexisting vessels, is essential for many physiological processes, such as pregnancy, embryonic development, and wound healing (1). However, uncontrolled or defective angiogenesis also contributes to many pathological processes, including tumor growth and metastasis (2).

Targeting angiogenesis is a promising strategy for the treatment of cancer. Tumor-associated blood vessels differ from vessels of normal tissue both structurally and functionally and can offer unique molecular targets for therapeutic interventions (3–5). There are several advantages to targeting the vasculature rather than the tumor cells proper. Tumor-associated vascular antigens are broadly expressed on cancers of different histological types, whereas they are generally absent or poorly expressed on most normal tissues (6–8). Immunotherapy may also elicit a significant bystander effect, because each capillary is thought to support hundreds of tumor cells and adaptive or antibody-mediated immune responses can easily access the tumor vasculature, whereas tumor islets may be compartmentalized and less accessible. Also, adaptive immunotherapy can persist, leaving a long-lasting memory response that protects the host against tumor recurrence. Finally, tumor cells are intrinsically more genetically unstable than vascular endothelial cells, and targeting them directly may promote tumor escape mechanisms (9).

Plasmid DNA offers a safe and promising method for vaccination and is approved for cancer immunotherapy for veterinary use (10). However, the immune responses induced to date by DNA vaccines in humans have been relatively weak compared with conventional vaccines, an issue that is particularly relevant for cancer vaccines because of the limited immunogenicity of tumor antigens. A combination of approaches are being studied to boost immune responses. In vivo electroporation of plasmid DNA or electrogene transfer increases DNA uptake, leading to enhanced expression in treated muscle and a concomitant increase in immune responses to the target antigen (11). The minimized domain of the C fragment of tetanus toxoid (TT) has been used to elicit antigen-specific immune responses (12). For example, DNA vectors encoding the tumor-associated antigen carcinoembryonic antigen (CEA) fused to TT can break tolerance to CEA and elicit significant antigen-specific $CD8^+$ T cell–mediated immune responses (13).

Human tumor endothelial marker 1 (TEM1; also known as endosialin or CD248) is overexpressed in the vasculature of carcinomas and brain tumors as well as in the vasculature and stroma of most sarcomas (14–17). Expression of TEM1 is variable among tumor types; it may be expressed on endothelial cells, pericytes, and fibroblasts in both mouse tumors (18) and human tumors (19, 20). Human *TEM1* gene expression is also induced by hypoxia under the regulation of HIF-2α (21). In the mouse, TEM1 is overexpressed during embryonic development, but is largely absent in adult tissue (18, 22). TEM1 is one of the most abundantly expressed tumor endothelial or stromal antigens in human tumors, making it a prime candidate for immunological targeting.

We hypothesized that effective DNA vaccination using TT as an adjuvant would be able to break tolerance to TEM1 and generate adaptive immunity targeted to the tumor vasculature. We propose that such vaccination can elicit potent antitumor activity in TEM1-expressing tumors by ablation of the tumor vasculature without affecting normal physiological functions that are dependent on angiogenesis. We tested these hypotheses by genetically fusing mouse *Tem1* cDNA with the first domain of fragment C of TT, creating a DNA vaccine (referred to herein as Tem1-TT) that we administered i.m. via electrogene transfer.

Authorship note: John G. Facciponte and Stefano Ugel contributed equally to this work.

Conflict of interest: The authors have declared that no conflict of interest exists.

Citation for this article: *J Clin Invest.* 2014;124(4):1497–1511. doi:10.1172/JCI67382.

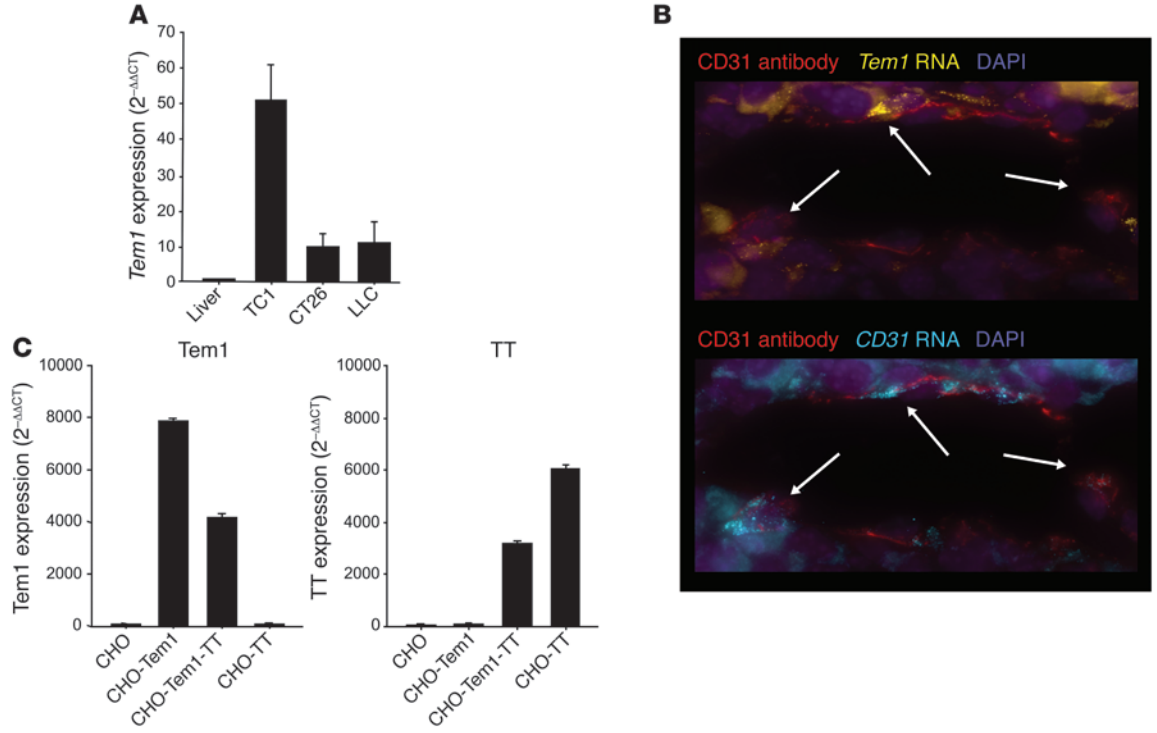

Figure 1

Physiological and plasmid DNA-induced TEM1 expression. (**A**) *Tem1* was expressed in tumors in vivo. qRT-PCR was performed with a *Tem1* probe. An *18S* probe was used as an endogenous control, and samples were normalized with mouse liver. Post–qRT-PCR calculations to analyze relative gene expression were performed by the $2^{-\Delta\Delta Ct}$ method. Error bars denote SD ($n = 5$). (**B**) *Tem1* RNA colocalized with CD31$^+$ cells. CT26 tumor sections were subjected to immunofluorescence with a CD31 antibody (red) and single-molecule RNA FISH for *Tem1* (yellow) or *CD31* (cyan). Bright spots in the RNA FISH channels correspond to individual transcript molecules. DAPI staining (purple) shows cell nuclei. Original magnification, ×100. Images shown are 85 μm wide. (**C**) Expression of the Tem1-TT DNA plasmid. A fusion Tem1-TT construct was generated by fusing codon-optimized *Tem1* cDNA (nt 1–2,297; aa 1–765) with the cDNA of the amino terminal domain of the fragment C of TT (819 bp, 273 aa). Expression of Tem1 or TT after transfection of the Tem1-TT construct was tested with CHO cells and assessed by qRT-PCR. Error bars denote SD ($n = 3$).

Results

DNA vaccination with Tem1-TT breaks tolerance to TEM1. Consistent with previous work in humans and mice, we found that *Tem1* was overexpressed in actively growing tumors of different background or histology (TC1, CT26, and LLC models) and was expressed at very low to undetectable levels in mouse normal tissues, as quantified by quantitative RT-PCR (qRT-PCR; Figure 1A and data not shown). In the hypervascularized CT26 mouse colon carcinoma model, *Tem1* mRNA was found to localize with, or to be in close juxtaposition to, *CD31* mRNA (Figure 1B and Supplemental Figure 1; supplemental material available online with this article; doi:10.1172/JCI67382DS1), which suggests that TEM1 is expressed by ECs and/or pericytes. These findings support the notion that TEM1 is an overexpressed vasculature-associated antigen in CT26 colon tumors, which can serve as a target for antitumor vascular therapy.

Using pcDNA3.1 as a DNA plasmid vector, the *Tem1* gene sequence was fused to the first domain of the C fragment of the TT sequence (TT 865–1,120) at its carboxyl terminal (see Methods). Expression levels of both sequences were measured by qRT-PCR after transient transfection of CHO cells (Figure 1C). This fusion construct was used to vaccinate healthy mice at 1-week intervals for a total of 3 immunizations. Splenocytes harvested from vaccinated mice were stimulated with a TEM1 peptide library consisting of 15 mers that overlap by 10 aa. The TEM1 library encompassing the entire protein sequence was divided into 4 pools: pool A (sequences spanning aa 1–197), pool B (aa 187–377), pool C (aa 367–557), and pool D (aa 547–765). This peptide-based approach facilitates the detection of CD8$^+$ and CD4$^+$ T cells that are specific for TEM1 sequences in the context of MHC class I and MHC class II, respectively (23). IFN-γ enzyme-linked immunosorbent spot assay (ELISpot) and intracellular staining (ICS) indicated that the majority of CD8$^+$ and CD4$^+$ T cell epitopes in BALB/c mice were contained within pool C (Figure 2A). Spleen-derived CD8$^+$ T cells from vaccinated C57BL/6 mice exhibited reactivity against pool D, whereas CD4$^+$ T cell responses were not detected (Figure 2B). As hypothesized, only the Tem1-TT DNA fusion vaccine was able to break tolerance to TEM1; specific responses were not detected in mice of either strain that were vaccinated with DNA encoding Tem1 or TT adjuvant alone.

To characterize the TEM1 sequences recognized by CD4$^+$ and CD8$^+$ T cells generated by the Tem1-TT vaccine, pools C and D were deconvoluted using a matrix scheme. For the BALB/c strain, pool C was further divided into minipools. TEM1-specific reactivity was found against minipools *f*, *g*, and *5* (Figure 2C). IFN-γ ICS analysis revealed that minipools *g* and *5*, corresponding to $TEM1_{516–530}$ (ITSATHPARSPPYQP), induced a stronger CD8$^+$ T cell response compared with minipools *f* and *5*, corresponding to $TEM1_{511–525}$ (GHKPGITSATHPARS). Both $TEM1_{516–530}$ and

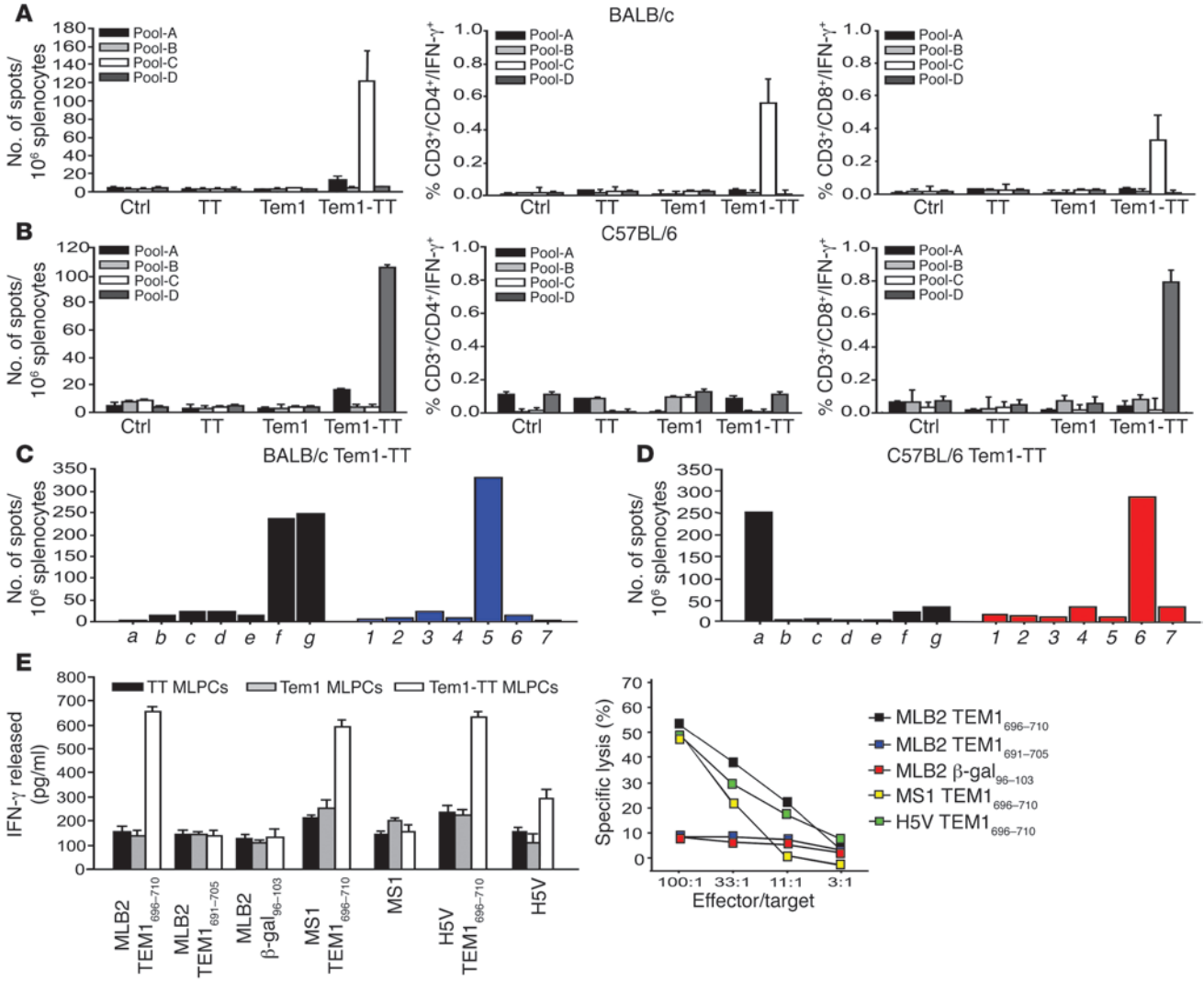

Figure 2

Characterization of TEM1 immunodominant epitopes. (**A** and **B**) Specific peptide pools restricted in H-2^d (**A**) and H-2^b (**B**) haplotypes. 1 × 10^6 splenocytes from BALB/c (**A**) or C57BL/6 (**B**) mice vaccinated with Tem1-TT were cultured with the 4 TEM1 peptide pools and tested by ELISpot and ICS for IFN-γ secretion. (**A**) Splenocytes from Tem1-TT–vaccinated BALB/c mice recognized pool C (left), which induced CD3$^+$CD4$^+$ (middle) and CD3$^+$CD8$^+$ (right) T cell responses. (**B**) Splenocytes from Tem1-TT–vaccinated C57BL/6 mice recognized pool D (left). By ICS, there was a specific CD3$^+$CD8$^+$ response (right). Data are mean ± SD (n = 5 per group) from 1 of 3 experiments. (**C** and **D**) Characterization of TEM1-derived peptides specific for H-2^d (**C**) and H-2^b (**D**) haplotypes. Peptides from pool C (**C**) or pool D (**D**) were divided into 7 minipools of 15 mers, so each individual peptide was present in 2 minipools and could be identified through an experimental matrix design. (**C**) Reactivity to pool C was present in minipools *f*, *g*, and *5*. (**D**) Reactivity to pool D was present in minipools *a* and *6*. Data are from 1 of 3 independent experiments. (**E**) TEM1$_{696–710}$ induced IFN-γ secretion and cytotoxic effector activity. Splenocytes from TT-, Tem1-, or Tem1-TT–vaccinated mice was used in peptide-stimulated cultures and tested in an IFN-γ secretion ELISA (left) and CTL assay (right). Tem1-TT exclusively primed and expanded antigen-specific CD8$^+$ T cells that killed ECs in the context of MHC class I/TEM1$_{696–710}$ peptide, but not control peptides.

TEM1$_{511–525}$ peptides stimulated a CD4$^+$ T cell response (data not shown). We therefore decided to use the TEM1$_{516–530}$ peptide for subsequent monitoring of the immune response in BALB/c mice. Using the same approach to further divide pool D into minipools for testing the C57BL/6 background, a specific TEM1 response was detected for minipools *a* and *6*, corresponding to the TEM1$_{696–710}$ peptide (GQSQRDDRWLLVALL) (Figure 2D). Using IFN-γ ICS, this sequence was found to specifically activate CD8$^+$ T cells (data not shown), which indicates that peptide TEM1$_{696–710}$ contains the immunodominant CD8$^+$ T cell epitope for C57BL/6 mice.

To confirm that the TEM1$_{696–710}$ peptide mediates target cell recognition and killing by CTL, splenocytes from vaccinated C57BL/6 mice were harvested and tested in mixed leukocyte peptide–stimulated culture (MLPC). MBL2 leukemia cells were used as the stimulatory cells. MLPCs were pulsed with TEM1$_{696–710}$ or control peptides for 5 days and tested for IFN-γ secretion by ELISA and in a ^{51}Cr cytotoxicity CTL assay. IFN-γ ELISA revealed that Tem1-TT vaccination selectively generated antigen-specific T cells that recognize the TEM1$_{696–710}$ peptide, but not the control peptides TEM1$_{691–705}$ or β-gal$_{96–103}$ (Figure 2E). Splenocytes from vaccinated C57BL/6 mice were also able to rec-

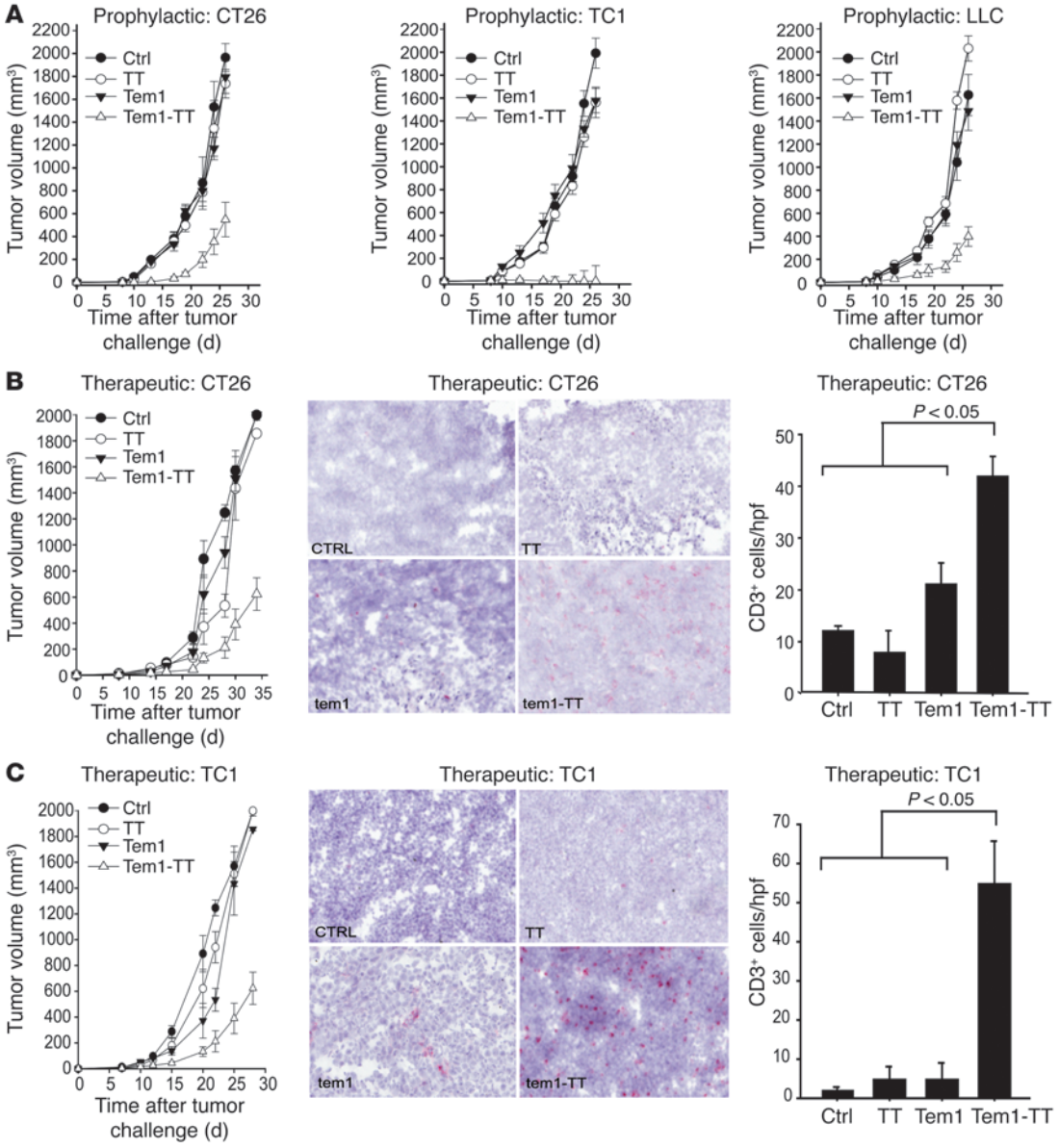

Figure 3

Tem1-TT vaccination controls tumor progression. (**A**) Tumor control in a prophylactic setting. BALB/c and C57BL/6 mice were immunized 3 times with Tem1, TT, or Tem1-TT vaccines, then injected s.c. with 1×10^5 CT26, TC1, or LLC cells. Data are mean ± SD (n = 10 per group) from 1 of 5 experiments. $P < 0.05$, Tem1-TT vs. Tem1 and Tem1-TT vs. TT (CT26, TC1, and LLC), pairwise multiple-comparison Tukey test. (**B** and **C**) Inhibition of CT26 and TC1 tumor progression and induction of $CD3^+$ T cell infiltration in a therapeutic setting. BALB/c mice were injected s.c. with 1×10^5 CT26 cells (**B**), and C57BL/6 mice were injected with 1×10^5 TC1 cells (**C**). Mice were immunized 1 day, 1 week, and 2 weeks later with Tem1, TT, or Tem1-TT vaccine and euthanized 33 (**B**) or 29 (**C**) days after tumor challenge. Left: Data points are mean ± SD (n = 10 mice/group) from 1 of 3 experiments. $P < 0.05$, Tem1-TT vs. Tem1 and Tem1-TT vs. TT (CT26 and TC1), Tukey test. $CD3^+$ T cells in corresponding tumor sections and quantification are also shown. Original magnification, ×20. Data are mean ± SD of a representative experiment (n = 5 per group).

ognize unpulsed or $TEM1_{696–710}$–pulsed H5V ECs, which express endogenous TEM1 protein, whereas MS1 ECs (which do not express TEM1; ref. 24) required TEM1 peptide pulsing to stimulate splenocytes from Tem1-TT–vaccinated mice (Figure 2E). In CTL assays, splenocytes from Tem1-TT–vaccinated mice efficiently lysed all 3 target cell types when pulsed with TEM1 peptide (Figure 2E). Together, these data suggest that Tem1-TT can break tolerance and elicit functional $CD8^+$ T cells that are specific for TEM1 epitopes. Furthermore, ECs can naturally process the endogenous TEM1 antigen and are able to present the cognate TEM1 peptide in an MHC class I–restricted fashion.

Tem1-TT DNA vaccine suppresses tumor growth and induces $CD3^+$ T cell tumor infiltration. To evaluate the ability of Tem1-TT vaccination to control tumor growth in vivo, we tested both prophylactic and therapeutic vaccine approaches using CT26, TC1, and LLC tumor models. Mice were vaccinated 3 times i.m. at weekly intervals, followed by tumor challenge (prophylactic), or tumor cells were inoculated first and then 3–5 days later were given 3 weekly

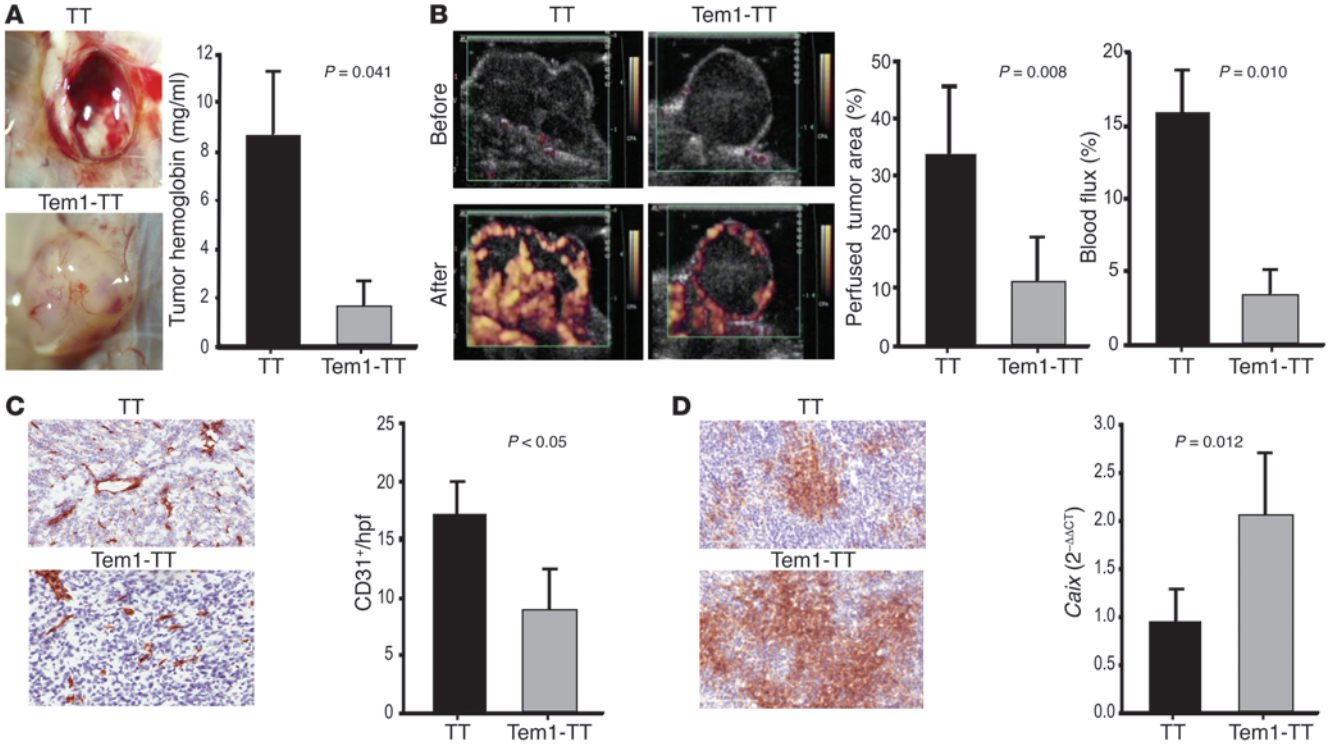

Figure 4

Tem1-TT vaccination inhibits CT26 tumor vascularization. (**A**) Tem1-TT vaccination reduced tumor hemoglobin content. Tumors at approximately 200 mm^3 were excised from TT- or Tem1-TT–vaccinated mice and inspected grossly. Tumors from Tem1-TT–vaccinated mice appeared pale relative to control tumors. Reduced hemoglobin levels in tumors from Tem1-TT–vaccinated mice were observed by ELISA. (**B**) Tem1-TT vaccine reduces tumor vascularity. Tumors from TT- or Tem1-TT–vaccinated mice were analyzed by Doppler ultrasound. Perfused tumor area and real blood flux are shown, measured and calculated by Doppler image analysis. (**C**) CT26 tumors from Tem1-TT–immunized mice had significantly decreased CD31 expression compared with TT vaccination. Also note the abnormal blood vessel shape. Original magnification, ×20. (**D**) CAIX expression was increased in tumors from Tem1-TT–immunized animals. CAIX expression was visualized by immunohistochemistry, and *Caix* was independently quantified by qRT-PCR in tumors from mice vaccinated with either TT or Tem1-TT. Original magnification, ×20. Data in **A**–**D** are mean ± SD of a representative experiment (n = 5 per group). Statistical analyses were performed with Student's t test.

vaccinations (therapeutic). Prophylactic treatment with Tem1-TT induced significant tumor protection compared with single Tem1 and TT constructs in all 3 tumor models (Figure 3A). These results reinforced the notion that the fusion construct Tem1-TT vaccine is essential to break TEM1 tolerance and generate protective immunity.

Therapeutic Tem1-TT vaccination conferred significant tumor protection compared with single construct controls in CT26 and TC1 tumor-bearing mice (Figure 3, B and C). Analysis of $CD3^+$ T cell tumor infiltration by immunohistochemistry revealed consistent, heavy infiltration of $CD3^+$ T cells after therapeutic vaccination with Tem1-TT within CT26 (42 ± 5 $CD3^+$ cells/high-powered field [hpf]; $P < 0.05$ vs. TT) and TC1 tumors (54 ± 11 $CD3^+$ cells/hpf; $P < 0.05$ vs. TT) compared with the single constructs and saline control (Figure 3, B and C). Cumulatively, these data indicate that the Tem1-TT vaccine induces significant T cell infiltration within tumors and exerts potent antitumor activity.

To demonstrate that the antitumor response by Tem1-TT vaccine is indeed immune mediated, and to determine whether the immune response is cellular or humoral in nature, we performed adoptive transfer of $CD3^+$ T cells or sera from Tem1-TT–immunized mice into TC1 tumor-bearing mice (Supplemental Figure 2). Splenocytes from Tem1-TT–immunized mice were enriched for $CD3^+$ cells and inoculated into naive mice. In simultaneous experiments, the serum from immunized mice was also transferred to naive mice. Mice were then sublethally irradiated and challenged with TC1 tumor. The antitumor response mediated by Tem1-TT vaccine was based on the induction of a $CD3^+$ T cell response, whereas serum had no therapeutic efficacy (Supplemental Figure 2). Therefore, although antibodies may be generated by the Tem1-TT vaccine, the results of our adoptive transfer experiments ruled out any humoral contribution to antitumor efficacy.

Tem1-TT vaccination inhibits tumor vascularization. To determine whether Tem1-TT vaccination controls tumor progression by targeting the tumor vasculature, we used common readouts for measuring the effects on the vasculature, but also measured the functional dynamics of the vasculature in the hypervascularized CT26 model (25). To ensure that tumors of the same size were studied, mice that were immunized with Tem1-TT were sacrificed 10 days later than mice immunized with TT vaccine, and available tumors were harvested. Tumors of similar volume (~200 mm^3) from both groups were assessed for tumor hemoglobin levels by ELISA, as a readout for blood perfusion. Tumors from mice vaccinated with Tem1-TT had significantly decreased hemoglobin levels compared with those of TT-vaccinated mice (Figure 4A), suggestive of reduced red blood cell perfusion in these tumors.

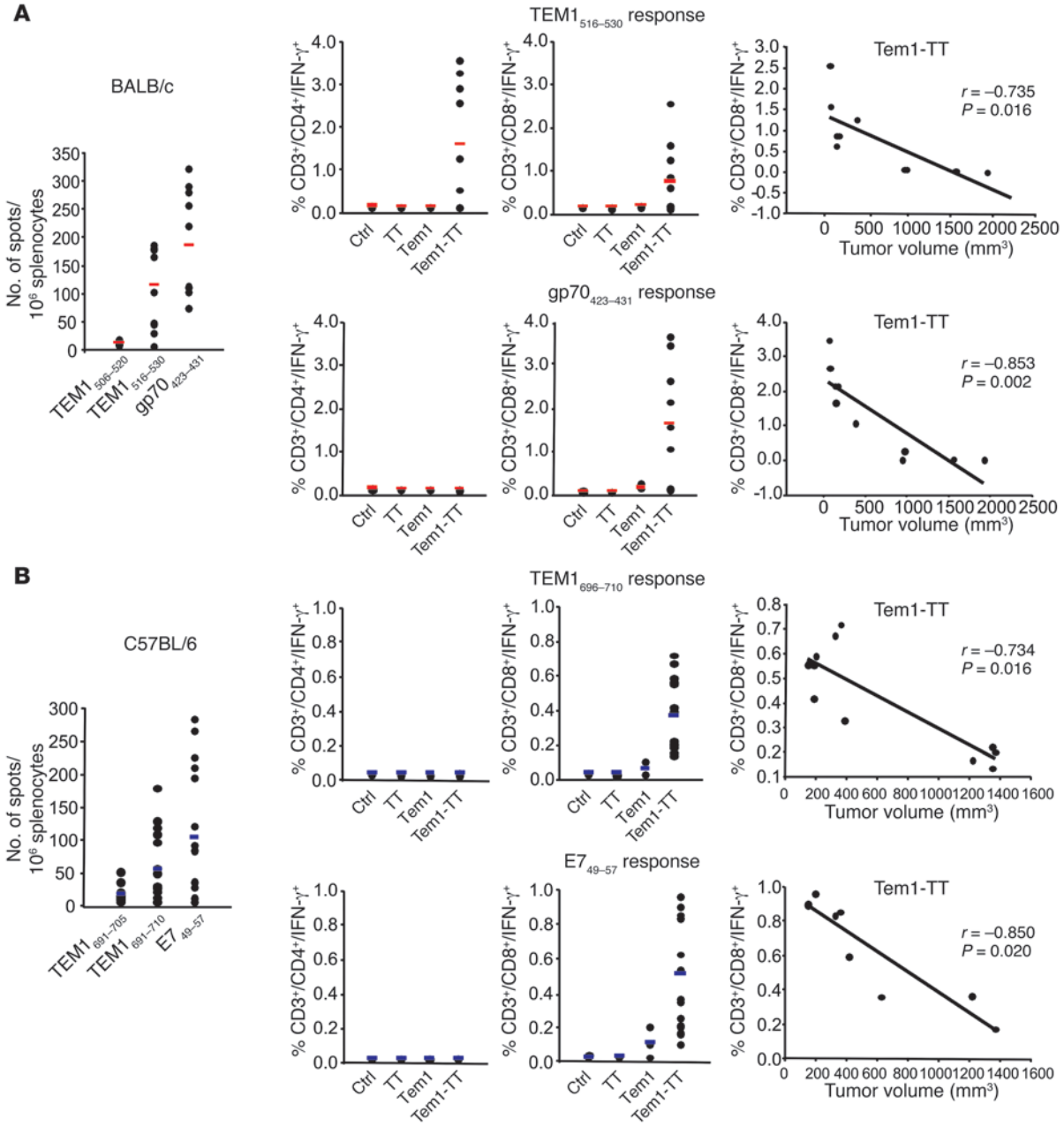

Figure 5

Tem1-TT vaccination induces secondary tumor cell–specific cytotoxic T cell responses in tumor-bearing mice. BALB/c (**A**) and C57BL/6 (**B**) mice were challenged, vaccinated, and euthanized as in Figure 3, B and C, respectively. 1×10^6 splenocytes from TT-, Tem1-, or Tem1-TT–vaccinated mice were tested for their capacity to respond to the specific TEM1 peptide ($TEM1_{516–530}$), and to AH1 antigen (**A**) or the TC1 tumor-associated E7 antigen (**B**). (**A**) Tem1-TT–vaccinated splenocytes mounted specific responses against the immunodominant peptide of TEM1 ($TEM1_{516–530}$) and the AH1 antigen, but not control peptide ($TEM1_{506–520}$), as measured by ELISpot. Tem1-TT induced $CD3^+CD4^+$ and $CD3^+CD8^+$ T cell responses against TEM1 antigen. The $CD3^+CD8^+$ T cell response from Tem1-TT–vaccinated mice correlated with suppression of tumor growth. ICS confirmed that Tem1-TT immunization induced an AH1-specific $CD3^+CD8^+$ T cell response that also correlated with tumor volume. (**B**) Splenocytes from mice vaccinated with Tem1-TT recognized $TEM1_{696–710}$ peptide and the E7 antigen, but not control peptide ($TEM1_{691–705}$). Only Tem1-TT vaccination was able to induce both a TEM1 and an E7 $CD3^+CD8^+$ T cell response, both of which correlated with tumor volume. Correlation analysis was performed by Spearman's rank correlation.

We then assessed the effects of Tem1-TT vaccination on the functional vasculature by measuring tumor vessel blood perfusion using ultrasound for each treatment group when tumors reached ~600 mm^3 in volume. Gas-filled microbubbles were injected i.v. and acted as a contrast agent as they flowed through the tumor blood vessels. Regions of perfusion in the tumors were visualized by ultrasound pulsing and contrast-enhanced Doppler imaging, which enabled us to determine the area of the tumor that was perfused (as a percentage of

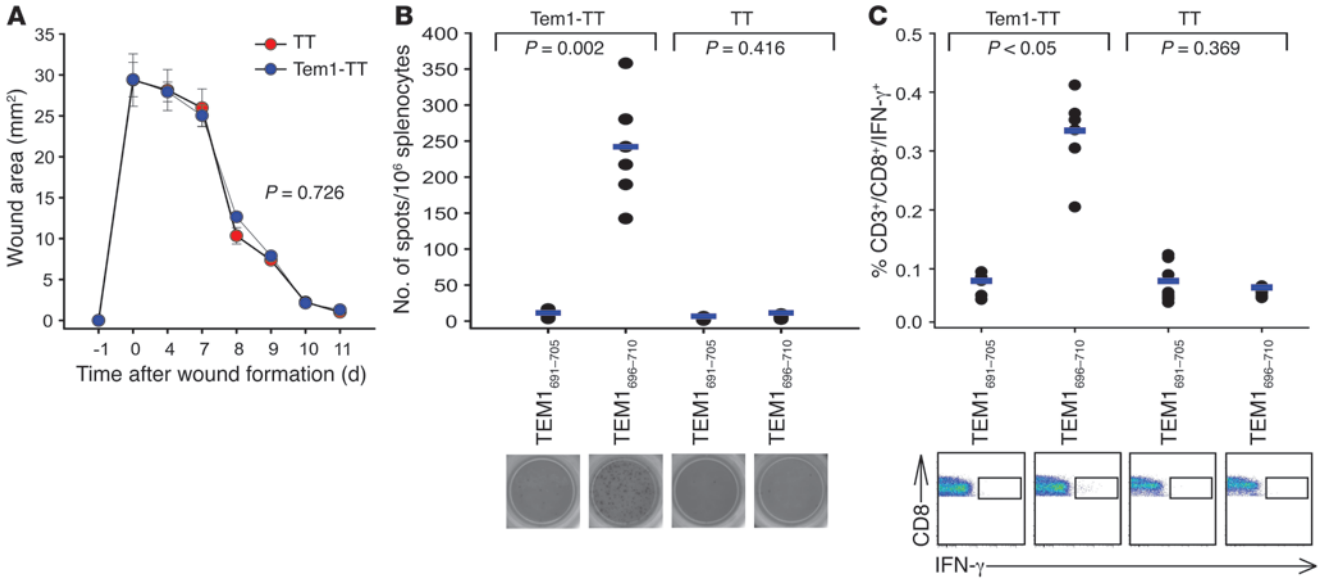

Figure 6

Wound healing is not delayed by Tem1-TT immunization. (**A**) Time course of wound healing. C57BL/6 mice were vaccinated 5 times with Tem1-TT or TT vaccine. 10 days after the final vaccination, 2 circular wounds were inflicted on the upper back of the mice. The wound area was measured every 2 days. Data are mean ± SD of 2 experiments (n = 10 per group for each experiment). P = 0.726, Tem1-TT vs. TT, pairwise multiple-comparison Tukey test. (**B** and **C**) TEM1-specific response. 20 days after the punch biopsies, mice were sacrificed to check the immune response against TEM1 antigen by IFN-γ ELISpot (**B**) and ICS (**C**) of bulk splenocytes (1×10^6). Statistical analyses were performed with Student's t test.

total tumor area) as well as the red blood cell flux (rate of blood flow) per unit area of the tissue (color-weighted fractional area) (26, 27). Contrast-enhanced images (after perfusion) showed a marked reduction in tumor perfusion (colored regions) in the Tem1-TT–treated group compared with TT-treated controls (Figure 4B). The reductions in both area of perfusion and blood flux in Tem1-TT–vaccinated tumors were statistically significant (P = 0.008 and P = 0.010, respectively; Figure 4B), which suggests that Tem1-TT vaccination disrupts the functional vasculature within the CT26 tumor.

We next assessed the apoptotic index of CT26 tumors by TUNEL assay. Compared with CT26 tumors from TT-immunized mice, cellular apoptosis increased in tumors from Tem1-TT–immunized mice (P = 0.014; Supplemental Figure 3A). We also observed colocalization of these apoptotic cells with the CD31 antigen (Supplemental Figure 3B), indicative of cell death of ECs of the tumor vasculature. Lastly, we also observed a reduction of cells positive for Ki-67, a marker for proliferating cells, within tumors from Tem1-TT– versus TT-immunized mice, which indicates that Tem1-TT vaccination lowers the proliferative capacity of the tumor, a likely consequence of disruption of the tumor vasculature (data not shown).

Next, the microvasculature density (MVD) of the tumors was measured by immunohistochemical staining of CD31. CT26 tumors from Tem1-TT–treated mice displayed reduced MVD compared with TT-treated tumors (Figure 4C). In addition to fewer $CD31^+$ ECs per hpf, structural disorganization of the vasculature was noted: Tem1-TT–treated tumor vessels appear flattened with less luminal space (Figure 4C), suggestive of vessel collapse as well as difficulty assembling new vasculature. Lastly, we tested whether reduced tumor perfusion in Tem1-TT–vaccinated mice was associated with an increase in tumor-associated hypoxia. Using immunohistochemistry, an increase in carbonic anhydrase IX (CAIX), a cellular biomarker of hypoxia, was observed in tumors of Tem1-TT– versus TT-vaccinated mice (Figure 4D). Analysis by qRT-PCR also showed an increase in *Caix* message levels in tumors from Tem1-TT–treated mice relative to controls (Figure 4D). These data suggest an association between reduced tumor blood perfusion and hypoxia in CT26 tumors from Tem1-TT–vaccinated mice.

Tem1-TT vaccination induces T cell responses against tumor-associated antigens as well as TEM1 antigen. Next, we tested whether immunization against TEM1 by Tem1-TT vaccine results in epitope spreading, an immunological phenomenon in which immunotherapy or chemotherapy kills tumor cells and induces cross-presentation of tumor-associated antigens followed by cross-priming (28, 29). Tumor antigen–specific vaccines can also induce epitope spreading, inducing specificity against antigens unrelated to the original vaccine target (30, 31).

We hypothesized that the antivascular effects described above would provide a rich source of dead or dying tumor/stromal cells capable of supporting a corollary cross-priming event that would generate immune responses to antigens other than TEM1. We used the immunodominant AH1 ($gp70_{423–431}$) peptide in the immunological assays. AH1 is the MHC class I–associated epitope for CT26 tumor, and as such, AH1-specific $CD8^+$ T cells can cure mice of established CT26 tumor (32, 33). AH1 peptide is derived from an endogenous retroviral gene product, gp70, expressed by CT26 cells (32). Splenocytes from CT26 tumor-bearing BALB/c mice vaccinated with Tem1-TT exhibited a specific response against $TEM1_{516–530}$ but not against the $TEM1_{506–520}$ control peptide, as expected, but they also exhibited a vigorous response against the AH1 peptide, as measured by IFN-γ ELISpot (Figure 5A). Tumor-bearing mice immunized with control TT vaccine did not respond to any of these peptides (data not shown). As measured by IFN-γ ICS, Tem1-TT vaccine induced

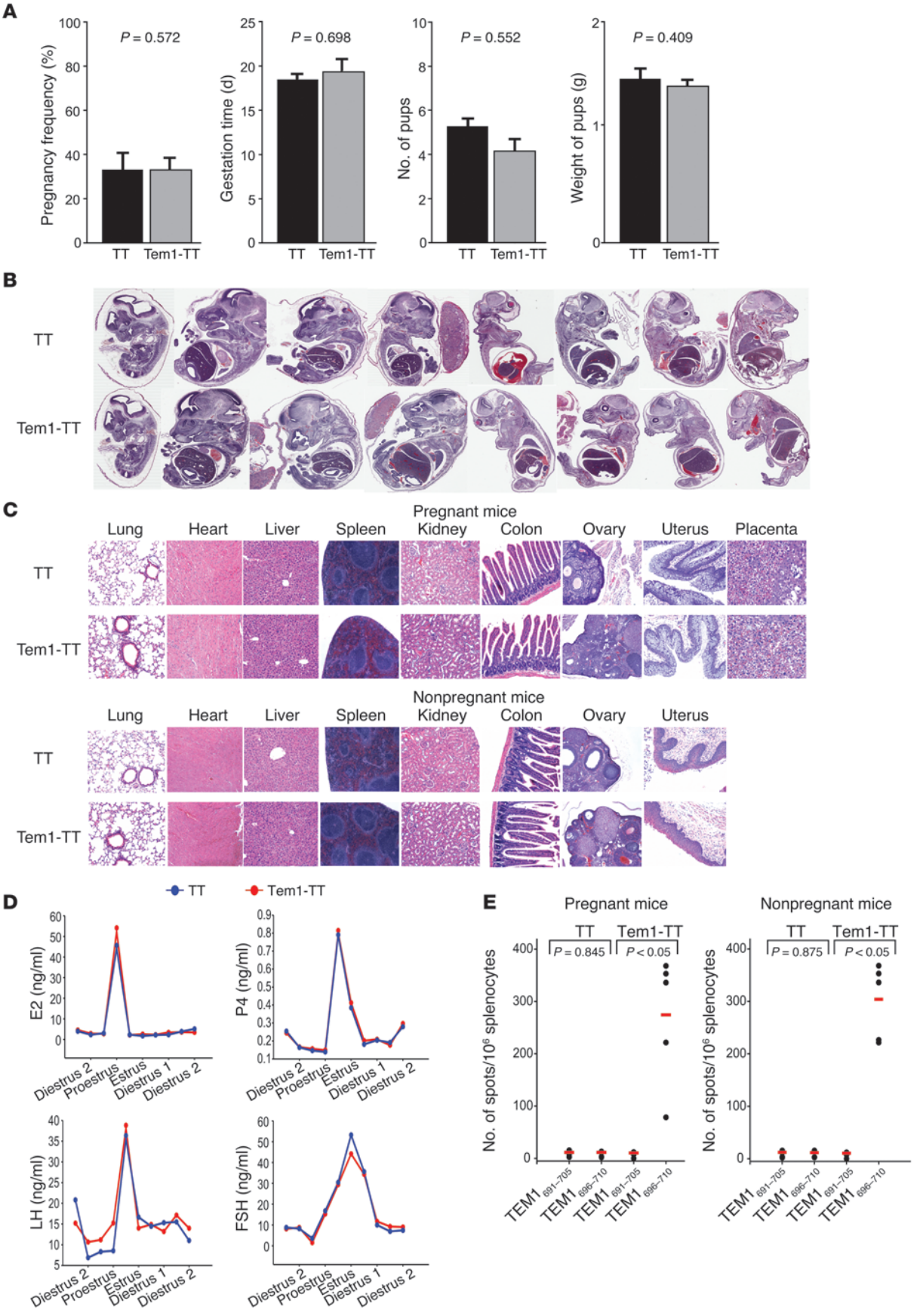
A
Pregnancy frequency (%)
P = 0.572
Gestation time (d)
P = 0.698
No. of pups
P = 0.552
Weight of pups (g)
P = 0.409
TT
Tem1-TT
B
TT
Tem1-TT
C
Pregnant mice
Lung
Heart
Liver
Spleen
Kidney
Colon
Ovary
Uterus
Placenta
Nonpregnant mice
D
E2 (ng/ml)
P4 (ng/ml)
LH (ng/ml)
FSH (ng/ml)
Diestrus 2
Proestrus
Estrus
Diestrus 1
E
No. of spots/10^6 splenocytes
P = 0.845
P < 0.05
P = 0.875
TEM1 691–705
TEM1 696–710

Figure 7
Tem1-TT vaccine does not affect reproduction. C57BL/6 female mice were vaccinated 5 times with Tem1-TT or TT vaccine followed by mating 1 week later. (**A**) Tem1-TT did not alter reproduction. Vaccination had no effect on fertility, gestation time, number of pups, or weight of pups (n = 15 per group). Data are representative of 2 independent experiments. Statistical analyses were performed with Student's t test. (**B**) Tem1-TT vaccine did not affect embryonic development. H&E staining of embryos of female mice vaccinated with TT and Tem1-TT showed no abnormalities detected for either group. (**C**) Tem1-TT vaccination did not induce tissue pathology. Histological analysis of lung, heart, liver, spleen, kidney, colon, ovary, uterus, and placenta from pregnant (postpartum) and nonpregnant mice (no placenta) revealed no pathological effects by either vaccine. Original magnification, ×10, except spleen and ovary (×4). (**D**) Tem1-TT vaccination did not affect the estrus cycle. In a separate independent experiment, sera from immunized mice had synchronized estrus cycles and were evaluated for reproductive hormones. No fluctuations were noted. (**E**) TEM1-specific T cell responses were unaltered by pregnancy. 1×10^6 splenocytes of vaccinated pregnant and nonpregnant mice were tested against $TEM1_{696–710}$ peptide or control peptide ($TEM1_{691–705}$) using IFN-γ ELISpot. Mice were boosted with a single injection of Tem1-TT or TT 45 days after the last immunization, then sacrificed 2 weeks later. There was significant recognition of $TEM1_{696–710}$ peptide by Tem1-TT– versus TT-vaccinated splenocytes from both pregnant and nonpregnant mice splenocytes (n = 5).

both $CD4^+$ and $CD8^+$ T cell responses against $TEM1_{516–530}$, while the response to AH1 was restricted to $CD8^+$ cells, as expected (Figure 5A). The frequency of the TEM1 $CD8^+$ T cell response from Tem1-TT–vaccinated mice was inversely correlated with tumor volume (Figure 5A), as was the $CD4^+$ T cell response (data not shown). A similar inverse correlation was found between the AH1-specific $CD8^+$ T cell response from Tem1-TT–vaccinated mice and tumor volume (Figure 5A).

To further understand the potency of the antivascular TEM1 response and the subsequent antitumor AH1 response, we performed adoptive T cell transfer from Tem1-TT–immunized naive or CT26 tumor–bearing mice to recipient mice that were challenged with CT26 tumor. $CD3^+$ T cells from Tem1-TT–immunized naive and tumor-bearing donor mice both significantly increased the survival of recipient mice injected with CT26 (Supplemental Figure 4, A and B). This result showed that the anti-TEM1 immune response generated by Tem1-TT in the non–tumor-bearing donor mice (without concomitant cross-priming and epitope spreading, as in the tumor-bearing mice) was sufficiently potent to control tumor growth, comparable to $CD3^+$ cells adoptively transferred from Tem1-TT–immunized tumor-bearing mice (Supplemental Figure 4, A and B). As expected, adoptively transferred $CD3^+$ cells from Tem1-TT–immunized naive mice exhibited a response against $TEM1_{516–530}$, but not against AH1 as in the tumor-bearing mice.

To confirm the epitope spreading phenomenon, we analyzed a second tumor model, TC1, a C57BL/6 epithelial lung tumor cell transformed by HPV E6 and E7 viral oncogenes. E7-derived peptide ($E7_{49–57}$) is the immunodominant epitope that can cure mice of established tumors (34). Mice immunized with Tem1-TT or control vaccine were challenged with TC1, as described previously. Splenocytes from Tem1-TT–vaccinated mice displayed $CD8^+$-specific immune responses against $TEM1_{696–710}$ peptide (but not the control peptide $TEM1_{691–705}$), as well as against the $E7_{49–57}$ epitope (Figure 5B). As we observed in the CT26 model, the frequency of both TEM1- and E7-specific $CD8^+$ immune responses correlated with TC1 tumor control (Figure 5B). Thus, effective Tem1-TT vaccination elicited a T cell–mediated response against both the tumor vasculature antigen (TEM1) and also against antigens expressed by the tumor cells themselves (gp70 and E7).

Tem1-TT vaccination does not affect wound healing or reproduction. Physiologic angiogenesis is critical for wound healing, and antiangiogenic agents such as bevacizumab have been associated with important safety concerns, including wound healing (35–37). We assessed whether wound repair was impaired by Tem1-TT immunization in C57BL/6 mice by wounding animals on their backs after immunization. There was no significant difference in time to wound closure between Tem1-TT– and control-vaccinated groups, despite generation of robust anti-TEM1 responses as measured by IFN-γ ELISpot and ICS (Figure 6, A–C).

Reproductive organs are sites of de novo angiogenesis, with both the corpus luteum and placenta being heavily dependent on formation of new blood vessels (38–40). Antiangiogenic compounds have been associated with defective luteogenesis, reproductive dysfunction, pregnancy loss, and teratogenesis (41–43). Previous studies have reported TEM1 expression in several tissues of the mouse embryo (22, 44). Postnatally, although TEM1 expression is downregulated in most organs, some expression persists in the renal glomerulus and in the adult uterus, where the expression pattern varies with the stage of the estrous cycle (45). Immunological targeting of the vascular TEM1 antigen could therefore have significant side effects on the reproductive system.

To test whether Tem1-TT immunization affects various aspects of mouse reproduction, female mice were immunized with Tem1-TT or TT vaccine and then mated (see Methods). Tem1-TT immunization had no effect on pregnancy success rate (P = 0.572), time to gestation (P = 0.698), total litter size (P = 0.552), and pup weight at birth (P = 0.409) compared with control immunization (Figure 7A). Furthermore, there were no anatomical or histological abnormalities in embryos from Tem1-TT– or control-immunized groups during early (E10) or late (E19) gestation (Figure 7B). We also assessed the potential effects of Tem1-TT immunization on various organs of vaccinated pregnant mice postpartum and found no abnormality in heart, lungs, liver, uterus, ovary, or placenta (Figure 7C). Similarly, organs from nonpregnant mice, including the uterus and the renal glomeruli, had no abnormalities after Tem1-TT immunization. To ensure that pregnancy did not dampen the effectiveness of Tem1-TT vaccination, we measured TEM1-specific T cell responses ($TEM1_{696–710}$) by IFN-γ ELISpot and ICS in the same female mice as above that were impregnated and gave birth, as well as in Tem1-TT–immunized mice that did not become pregnant after vaccination (Figure 7E and Supplemental Figure 5). TEM1 responses were roughly equal between pregnant and nonpregnant mice that were Tem1-TT immunized (Figure 7E). The ICS assay similarly showed that the TEM1 response was roughly of equal frequency between pregnant and nonpregnant mice and $CD8^+$ specific (Supplemental Figure 5), as expected with this TEM1 peptide.

Lastly, because antiangiogenic agents may disrupt luteogenesis (38, 46, 47), we also tested reproductive endocrine function after Tem1-TT vaccination in a separate independent experiment. Mice were vaccinated only, then had their estrous cycle synchronized by medroxyprogesterone, and serum levels of 17β-estradiol (E2), progesterone (P4), luteinizing hormone (LH), and follicle-stimulating hormone (FSH) were measured longitudinally. Patterns of E2, P4, FSH, and LH expression were similar between TT- and

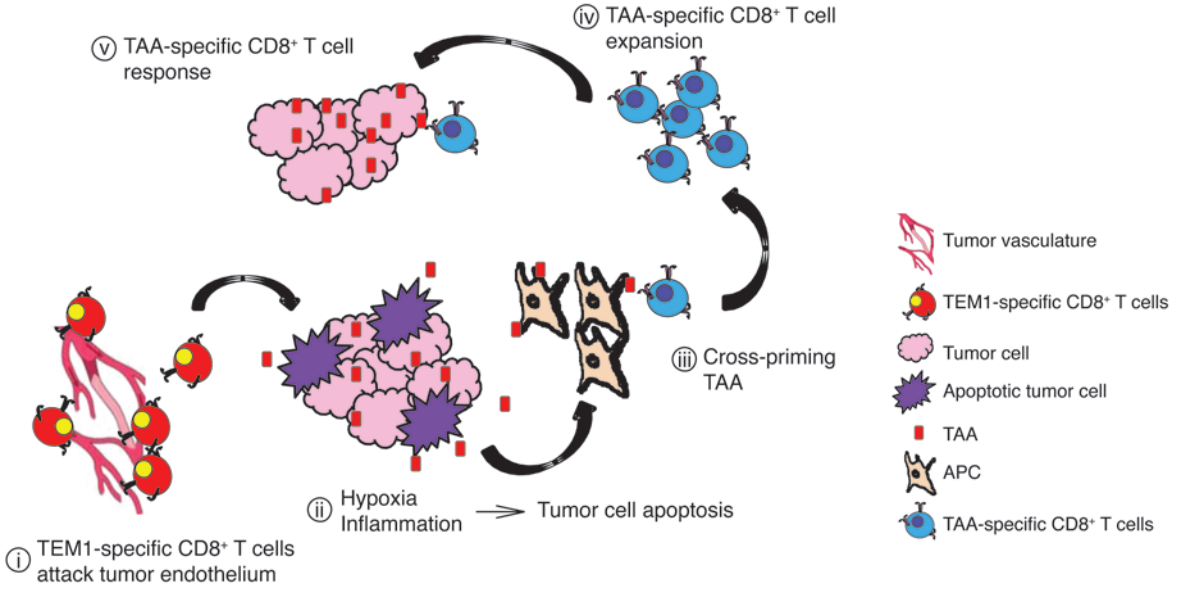

Figure 8

Proposed mechanism of action of Tem1-TT vaccination. (i) Tem1-TT vaccine induces expansion of TEM1-specific CD8+ T cells that target the CT26 tumor vasculature. These cytolytic effectors target and kill TEM1-expressing cells, most likely tumor-associated endothelial cells and/or pericytes. (ii) This event results in reduction of the tumor vasculature, inducing inflammation and tumor hypoxia, which results in localized tumor cell death. (iii) Dead tumor cells are scavenged by APCs, which process relevant tumor-associated antigens (TAA; e.g., AH1 antigen in CT26 tumor model). (iv) This cross-presentation event results in a secondary cross-priming event that expands tumor-specific cytotoxic CD8+ T cells to tumor cell–derived epitopes. (v) Tumor-specific cytotoxic CD8+ T cells lyse and eliminate tumor cells, resulting in control of tumor growth.

Tem1-TT–vaccinated groups (Figure 7D); therefore, Tem1-TT did not modulate hormone levels during estrus. Collectively, Tem1-TT vaccination appears to have no untoward effects on physiological processes in mice that depend on de novo angiogenesis.

Discussion

Tumor vasculature is critical for tumor growth and presents unique immunological epitopes, becoming an attractive target for therapy. Although many antiangiogenic and vascular-disrupting therapeutic approaches have been developed, immunotherapy offers the unique advantage of protective memory. Active immunization against whole tumor–derived ECs has produced encouraging preclinical results, but is not practical (48–50). Development of active vaccination targeting vascular epitopes has been previously reported, but safety has not been adequately addressed (31, 51). In some experiments using adoptive therapy of T cells engineered to recognize the vascular growth factor 2 receptor, there was severe dose-dependent toxicity (52). Thus, identification of unique epitopes on the tumor vasculature that are suitable for immunotherapy is of high significance for the tumor immunology field. TEM1 is a surface protein expressed by tumor endothelial and endothelial progenitor cells (53) as well as pericytes and tumor-associated fibroblasts (19, 54, 55) and is found in the vasculature of tumors (4, 14, 56–61), but not in normal vessels (57, 58). TEM1 is implicated in vascular cell adhesion, migration, development (62, 63), neoangiogenesis (57, 58), and tumor progression (20), and its overexpression is associated with poor survival (61). Importantly, *Tem1*$^{-/-}$ mice were previously shown to resist tumor growth, invasiveness, and metastasis, but were otherwise healthy and exhibited normal wound healing (64). Thus, knockout of TEM1 greatly attenuated tumor establishment and progression, without affecting physiologic angiogenesis. However, whether this null phenotype can be reproduced through therapeutic means is not known. We showed here for the first time that effective immunization against TEM1 closely phenocopied the *Tem1*$^{-/-}$ mouse, severely prohibiting the establishment of tumors and inhibiting the progression of tumor growth without affecting reproduction and/or would healing.

We developed a DNA vaccine that expresses the full-length mouse *Tem1* cDNA fused to TT adjuvant. Immunization with the Tem1-TT vaccine reduced tumor vasculature compared with mice given control vaccine, as measured by MVD, functional imaging (ultrasound imaging of blood perfusion and blood flux), and hematocrit levels and indirectly supported by increased levels of CAIX in the tumor, suggestive of localized hypoxia therein. Splenocytes from Tem1-TT–vaccinated mice actively secreted IFN-γ and lysed TEM1-expressing ECs in vitro and specifically induced a cellular immune response that controlled tumor progression. Cumulatively, these findings indicate that vaccination with Tem1-TT specifically targets the TEM1-expressing cells of the vascular system and can functionally disrupt the tumor vasculature.

Breaking tolerance to TEM1 with DNA vaccine required the fusion of *Tem1* and TT genes. TT may enhance immunogenicity through several mechanisms; the whole C fragment of TT activates DCs to secrete cytokines involved in CD4+ T cell activation (11, 65). In addition, fragment C contains universal T helper epitopes (p30, p2), which are effective across different MHC class II haplotypes in mice and humans and elicit strong CD4+ responses (66). Peptides within domain 2 of fragment C are strong CD8+ CTL epitopes, which may compete with the fusion peptides. Elimination of domain 2 enhances CTL responses to fused peptides (67), and thus we eliminated it from our TT con-

struct accordingly. In addition, we generated localized inflammation by in vivo electrogene therapy during both prime and boost injections. Electrogene therapy enhances responsiveness (68, 69) and has facilitated translation of DNA vaccines into clinical trials (12, 70, 71). All of these attributes may be contributing to the generation of potent anti-TEM1 immune responses we observed with Tem1-TT immunization.

Our approach used full-length antigen rather than peptide, thus bypassing a major limitation of peptide-based cancer vaccines, namely MHC restriction. Genetic fusion of TT to the 3′ end of full-length antigens has been tested previously by us and others (13, 72). Our DNA vaccine elicited $CD4^+$ and $CD8^+$ anti-TEM1 responses in the BALB/c mouse and a $CD8^+$ response in the C57BL/6 mouse. Given the prime/boost approach we used, it is likely that the responses observed are directed against the immunodominant TEM1 epitopes in each mouse strain (11, 73). Other adjuvant formulations may identify alternative dominant and/or subdominant epitopes.

In previous mouse studies, DNA vaccination with the tumor-associated antigens AH1 and E7 induced $CD8^+$ cell–dependent regression of established tumors that expressed those antigens (33, 74). In the studies presented here, fusion of the TEM1 antigen to the TT adjuvant increased the immunogenicity of the target antigen and the efficacy of tumor control. It also generated robust CTL activity against tumor cell proper immunodominant epitopes, such as AH1 and E7. This was not achieved by direct targeting of these antigens, but rather indirectly by targeting the vasculature antigen TEM1. Taken together, our data suggest a model whereby Tem1-TT vaccination induces expansion of TEM1-specific T lymphocytes (Figure 8). These effector T cells target TEM1-expressing cells in the tumor vasculature, including tumor-associated ECs and/or pericytes. This immune attack impairs the tumor vasculature, with increases in local tumor-associated hypoxia and likely inflammation-related mediators, resulting in apoptosis of local tumor cells. These apoptotic bodies are scavenged by macrophages and DCs that process and present additional tumor-associated antigens. This secondary cross-priming event then expands tumor-specific cytotoxic $CD8^+$ T cells, which work hand in hand with the anti-TEM1 immune response to eradicate larger numbers of tumor cells, resulting in improved control of tumor growth. The anti-TEM1 response and the antitumor immune responses against AH1 and E7 significantly correlated with control of tumor growth. Further studies will address the kinetics of the TEM1 and AH1 immune response. Our findings are consistent with the general paradigm of epitope spreading as a mechanism underlying superior immunotherapeutic outcomes and extend this concept to include T cell specificities against tumor-associated vasculature antigens (75).

The results of our adoptive transfer experiments (Supplemental Figure 2) suggest that tumor control by Tem1-TT vaccination is mediated primarily by $CD3^+$ cells, while serum (containing antibodies) does not play any major therapeutic role. We did not directly measure anti-TEM1 antibodies potentially generated by Tem1-TT, and therefore cannot entirely rule out the possibility that anti-TEM1 antibodies contribute to the observed efficacy of Tem1-TT vaccine in some capacity. Adoptive cell transfer also illustrated the effective generation of memory responses: mice challenged with tumor 6 months after adoptive transfer of $CD8^+$ T cells remained tumor free (data not shown), which illustrated that Tem1-TT generated robust, long-lasting adaptive immune responses. The adoptive transfer experiments with the CT26 model showed that Tem1-TT vaccination generated TEM1-specific $CD3^+$ T cells that, on their own, could directly delay tumor growth and confer survival advantage to mice. These data also showed that Tem1-TT vaccination generated a dually specific T cell response, with a primary TEM1-specific response targeting the tumor vasculature generated by Tem1-TT vaccine, and a secondary response targeting the tumor cell–specific antigen AH1 generated by epitope spreading.

An ideal tumor vasculature antigen is one that is overexpressed in tumors and poorly expressed in peripheral tissues. Expression of TEM1 in the mouse is spatiotemporally regulated. By using a lacZ knockin model, *Tem1* gene expression was initially detectable in the kidney of prenatal embryos (45). Postnatally, *Tem1* expression decreases in most organs, but persists in the renal glomerulus and in the adult mouse uterus. In mice immunized with Tem1-TT, we did not observe toxicity in association with angiogenic processes, such as reproduction or wound healing. It is perhaps surprising that the Tem1-TT vaccine could mediate tumor vessel destruction without causing significant toxicity during pregnancy and wound healing. However, angiogenesis during tumor development differs significantly from the uterine NK cell–driven angiogenesis seen during implantation and placenta development (76, 77) and from the highly organized, slow growth of wound healing. In addition, tissue specificity and cells involved in tumor vessel recruitment differ from superficial wounds, although many similarities exist (78).

Cumulatively, our data indicated that immunization with a DNA vaccine encoding Tem1-TT induces TEM1-specific cell-mediated immune responses, disrupts the tumor vasculature, and controls tumor growth without affecting important normal physiological functions. Our preclinical data set can serve as a foundation for clinical studies targeting human TEM1 tumor vasculature antigen.

Methods

Mouse strains and cell lines. 8-week-old C57BL/6 (H-2^b) and BALB/c (H-2^d) mice were purchased from Charles River. Lung tumor cell line TC1 transformed by HPV E6 and E7 viral oncogenes (H-2^b), lung carcinoma line LLC (H-2^b), colon carcinoma line CT26 (H-2^d), leukemia cell line MBL2 (H-2^b), and EC lines MS1 (H-2^b) and H5V (H-2^b) were cultured in RPMI 1640 (Cellgro; catalog no. 10-104-CV) or DMEM (Cellgro; catalog no. 40-101-CV) medium supplemented with 2 mM L-glutamine and 150 U/ml streptomycin plus 200 U/ml penicillin (Cellgro; catalog no. 30-0010CI) and 10% heat-inactivated FBS (Gibco; catalog no. 35-010-CV).

DNA vectors and immunization procedures. The vaccine construct was generated by fusing mouse *Tem1* cDNA (nt 1–2,297; aa 1–765) with the cDNA of the aminoterminal domain of fragment C of TT. The TT fragment DNA was introduced at the 3′ end of the *Tem1* coding sequence, generating the plasmid pcDNA3.1/Tem1-TT. The codon usage-optimized cDNA of Tem1-TT was synthesized by oligonucleotide assembly (GeneArt; Life Technologies). All constructs were routinely sequenced by the DNA sequencing core facility at University of Pennsylvania, and Tem1 and TT constructs were confirmed with the correct sequences. DNA immunization was performed as described previously (79). Briefly, 50 μg plasmid in saline was injected i.m., and electrogene transfer was performed (2 pulses at 100 mV for 200 ms) immediately after injection. In Figure 3A (prophylactic setting), mice were euthanized when tumors reached approximately 2,000 mm^3.

RNA isolation and qRT-PCR. Total RNA was isolated from 100–500 mg frozen organs or tumors with TRIZOL reagent (Invitrogen; catalog no. 15596-018). After treatment with RNase-free DNase (Invitrogen; catalog no. AM2222),

RNA was reprecipitated, quantified by spectrophotometry, and analyzed for RNA integrity by gel or Bioanalyzer. Total RNA was reverse transcribed using the Superscript First-Strand Synthesis Kit (Invitrogen; catalog no. 10928-042) for RT-PCR under conditions described by the supplier. qRT-PCR was performed with inventoried mouse *Tem1* probe (ABI Biosystems; catalog no. Mm00547485) as well as *18S* probe as an endogenous control (4310893E-0710037). Samples for *Tem1* expression in mouse organs were normalized using mouse liver as a calibrator. RNA isolated from tumor was used to set up qRT-PCR, with mouse *Caix* as a probe, as well as *18S* probe as an endogenous control. To monitor TEM1 expression in transfected cells, CHO cells were transfected with 1 μg Tem1-TT plasmid or single constructs in a 6-well dish. After 48 hours of incubation, whole-cell lysates were harvested, and total mRNA was extracted using TRIzol. The Tem1 and TT RNA present in the cell lysates was detected by qRT-PCR with custom primers for optimized Tem1 and optimized TT, as designed by ABI Biosystems by PrimerExpress. Post–qRT-PCR analysis to quantitate relative gene expression was performed by the comparative Ct method ($2^{-\Delta\Delta Ct}$). Error bars denote SD (n = 3) unless otherwise indicated.

RNA FISH. Frozen tissue was sectioned onto poly-L-lysine–coated coverglasses (BD Biocoat; catalog no. 354085), fixed in formaldehyde, permeabilized, and stored in 70% ethanol. The single molecule RNA-FISH protocol was carried out as described previously (80). Samples were hybridized to the FISH probes overnight at 37°C in 2× SSC with 10% (v/v) formamide (Ambion; catalog no. AM9342) and 10% (w/v) dextran sulfate (Sigma-Aldrich; catalog no. D8906). For *Tem1* and *CD31*, probe mixtures consisted of 48 20-mer DNA oligonucleotides (Biosearch Technologies) each, designed to tile their respective coding sequences, and coupled to Cy5 (*Tem1*) and Cy3 (*CD31*). After washing with PBS to remove unbound probe and storage for a few days, samples were stained for CD31 by overnight incubation with biotin-conjugated rat anti-mouse CD31 (BD Biosciences — Pharmingen; clone MEC13.3) at 4°C in PBS (1:250 dilution) and a 20-minute incubation with FITC-labeled streptavidin (BD Biosciences — Pharmingen; catalog no. 554060) at 4°C in PBS. Samples were mounted in a glucose oxidase–based 2× SSC antifade buffer (Sigma-Aldrich; catalog no. G2133) and imaged on a conventional wide-field epifluorescence microscope (Nikon Eclipse Ti) with a ×100 1.4 NA oil immersion objective. Image stacks were acquired with 0.35-μm vertical spacing and collapsed into single 2D images by maximum projection.

Synthetic peptides. A mouse TEM1 peptide library of 151 peptides generated as 15 mers overlapping by 10 aa was synthesized by Mimotopes and dissolved in DMSO at approximately 20 mg/ml. Pools, minipools, and individual peptides were used at 2 μg/ml. kb-restricted $TEM1_{691–705}$ peptide (ESGLAGQSQRDDRWL), $TEM1_{696–710}$ peptide (GQSQRDDRWLLVALL), E7 peptide (RAHYNIVTF), β-gal (DAPIYTNV) and Ld-restricted $TEM1_{506–520}$ peptide (PDLPFGHKPGITSAT), $TEM1_{516–530}$ peptide (ITSATHPARSPPYQP), and AH1 peptide (SPSYVYHQF) were all synthesized by JPT. The 151 15-mer peptides were divided into pools A–D, with approximately 40 peptides each (pool D contained fewer peptides), to identify immunoreactive peptides (Figure 2, A and B). Once immunoreactive pools were identified, peptides from pools C and D (Figure 2, C and D) were divided into 7 minipools of 15 mers, so each individual peptide was present in 2 minipools and could be identified through an experimental 7×7 matrix design (23).

ELISpot. 96-well MAIP plates (Millipore; catalog no. N4510) were coated overnight with a 2.5 μg/ml solution of rat anti-mouse IFN-γ (BD Biosciences — Pharmingen; catalog no. 551216). Bulk splenocytes were plated at 1×10^6 cells/well in triplicate and incubated for 20 hours at 37°C with 2 μg/ml peptides. After incubation, plates were washed with PBS and 0.05% Tween 20 (Bio-Rad; catalog no. 170-6531) and incubated overnight at 4°C with anti-mouse biotin-conjugated anti–IFN-γ antibody (BD Biosciences — Pharmingen; catalog no. 551506). The following day, streptavidin-alkaline phosphatase conjugate (BD Biosciences — Pharmingen; catalog no. 554065) was added for 30 minutes. Plates were developed by adding nitroblue tetrazolium/5-bromo-4-chloro-3-indolyl phosphate (Pierce), and spots were then counted using an automated ELISpot reader (Autoimmun Diagnostika GmbH).

ICS for IFN-γ. 5×10^6 mouse splenocytes in 1 ml RPMI with 10% FCS were incubated with the indicated peptides (final concentration of each peptide, 1 μg/ml) and 1 μg/ml brefeldin A (BD Biosciences — Pharmingen) at 37°C for 12–16 hours as previously described (81). Cells were washed, stained with surface antibodies, fixed, permeabilized, and incubated with FITC-labeled IFN-γ antibody (BD Biosciences — Pharmingen; catalog no. 554411). Cells were fixed with 1% formaldehyde solution in PBS and analyzed on a FACSCanto flow cytometer using Flowjo software (Treestar).

MLPCs. MLPCs were set up with 5×10^6 splenocytes from vaccinated mice stimulated in vitro with 1 μg/ml specific peptide. The culture was incubated for 5 days in DMEM with 10% FBS at 37°C in 5% CO_2.

ELISA. 10^5 splenocytes from MLPCs were restimulated for 24 hours in triplicate with an equal number of target cells, supernatants were harvested, and IFN-γ secretion was measured by ELISA (Biolegend). Serum from vaccinated mice was evaluated by ELISA to check the level of P4 (Enzo; catalog no. ADI-900-011), E2 (Enzo; catalog no. ADI-900-008), LH (Uscnk), and FSH (Uscnk). Mouse hemoglobin ELISA kit was obtained from Kamiya Biomedicals. Briefly, 100 mg fresh tumor was lysed with 200 μl RIPA buffer. Mouse hemoglobin quantification was performed according to the manufacturer's protocol with 2 μg/ml tumor lysate. Reading results were interpolated to test sample values from fitted calibration curve of mHgb serial dilutions. Each value represents the mean of triplicates from a mouse tumor. Representative results of 3 independent measurements are shown from 5 mice per group.

Cytotoxicity assay. Cytotoxicity was measured by ^{51}Cr release assay. MLPCs were incubated with MBL2 cells, MS1 cells, or H5V cells that were unpulsed or pulsed with the $TEM1_{696–710}$ peptide. Target cells were labeled with 100 μCi ^{51}Cr (Amersham) before being mixed with effector cells. Assays were performed in triplicate, and supernatants were harvested to measure ^{51}Cr released. Specific lysis was calculated from triplicate samples as (experimental cpm – spontaneous cpm)/(maximal cpm – spontaneous cpm) and expressed as a percentage.

Immunohistochemical tumor analysis. CAIX, CD31, and CD3 were detected by immunohistochemistry in solid tumors. Tumors were embedded in OCT medium and immediately snap frozen in dry ice. Sections (6 μm thick) were stained for mouse CAIX (R&D Systems; catalog no. AF2344, DAB chromogen), CD31 (BD Biosciences — Pharmingen; clone 390, catalog no. 558737, DAB chromogen), and CD3 (BD Biosciences — Pharmingen; clone 15.5-2C11, catalog no. 550275, DAB chromogen) with hematoxylin as a counterstain. For TUNEL assay, frozen sections (6 μm thick) of the OCT-embedded tissue were air dried for 30 minutes under the hood and fixed with 2% paraformaldehyde in PBS for 30 minutes at room temperature. Each slice was treated with 100 μl of 3% H_2O_2-methanol solution for 20 minutes at room temperature and washed 3 times in PBS. To cover the nonspecific binding sites, each slice was treated with 10% normal goat serum blocking solution for 1 hour at room temperature. Tissue sections were incubated overnight at 4°C with rat anti-mouse CD31 primary antibody (1:200 dilution; BD Biosciences — Pharmingen; catalog no. 550274). After washing 3 times in PBS, the slices were incubated with Texas Red goat anti-rat IgG secondary antibody (1:500 dilution; Vector Laboratories; catalog no. TI-9400) at room temperature for 1 hour. To identify the apoptotic dead cells in situ, TUNEL was performed with Cell Death Detection Kit (Roche Applied Science; catalog no. 11684809910) according to the manufacturer's instructions. Images of the slides were taken using a Nikon Ti fluorescence microscope and a Leica TCS SP8 confocal microscope.

Ultrasound analysis of tumor vasculature. Lipid-coated microspheres filled with gas (Definity Lantheus Medical Imaging Inc.) were used as contrast agent with power Doppler imaging to visualize the regions of perfusion in the tumor. In brief, CT26 tumor-bearing mice (tumor volume, ~600 mm^3) were anesthetized and injected with 0.02 ml octafluoropropane gas (Definity Lantheus Medical Imaging), and power Doppler imaging was performed using a broadband 7- to 15-MHz probe (HDI500 SonoCT; Philips). Power Doppler images were acquired at a frame rate of 0.5 Hz to minimize microbubble destruction by the imaging ultrasound pulses. The Doppler signal from the inflowing contrast agent was visible in the images in color superimposed on the grayscale image of the tumor. Contrast-enhanced power Doppler imaging was performed as described previously (26). The power Doppler images at peak enhancement were analyzed to determine percentage area of the tumor with flow (percentage perfused area). The perfused tumor area for each treated group was calculated as the ratio of the area resolution by the contrast agent to the total tumor area in a single plane. Color-weighted fractional area of the colored pixels within the region of interest was measured as described previously (82). The color of each pixel in the contrast-enhanced power Doppler image measures the fractional volume of the contrast flowing through the pixel, and the color-weighted fractional area (product of color level and fraction area covered by colored pixels) measures the contrast volume per unit area of tumor (blood flux) (83).

Histologic evaluation of embryo and tissues in vaccinated mice. Several organs (liver, lungs, small and large bowel, kidneys, heart, testis, brain, and spleen) and embryos at different time points (E10 and E19) were collected to assess for possible treatment toxicity. Tissues were fixed in 10% buffered formalin and embedded in paraffin. Histopathologic evaluation was performed on standard H&E sections.

Reproduction and wound-healing assay. To test whether Tem1-TT immunization affects mouse pregnancy by interfering with prenatal angiogenic processes, 6- to 8-week-old female mice were immunized 5 times as previously described (79). 1 week after the last immunization, mice were mated for 48 hours with individually housed males. Coitus was monitored the following morning and confirmed by the presence of a vaginal plug. Half the mice were used to measure time to gestation, pup weight at birth, and total litter size. The other pregnant mice were used to check for gross abnormalities of the embryos at E10 and E19 at the whole-animal level as well as at the organ level. For ELISpot and ICS (Figure 7E and Supplemental Figure 5), 45 days after the last immunization, the pregnant mice above that gave birth to pups (for time to gestation and pup weight at birth) and nonpregnant mice were boosted with a single injection of Tem1-TT or TT DNA. 2 weeks later, mice were sacrificed to assess the immune response against TEM1 antigen in both assays.

We also performed a separate independent experiment to measure the effects of Tem1-TT on the estrus cycle. Mice were immunized once per week for 4 weeks. To synchronize the estrus cycle, female mice were then treated s.c. every day with 2 mg medroxyprogesterone (Sigma-Aldrich; catalog no. M6013), beginning 3 days after the final vaccination (84). After the last drug treatment, mice were sacrificed every 12 hours for 5 days. Serum was collected (3 mice per group pooled per time point) to check blood hormone levels.

The wound-healing assay used in this study was done according to previously described methods (85). Briefly, 7 days after the last immunization with DNA vaccine, mice were anesthetized, hair was removed, and skin was cleaned with an aseptic wipe. 2 circular defects were outlined using a fine-tipped marking pen. The defect was created by elevating the skin and panniculus carnosus in the center of the outlined defect using forceps, followed by excision of the outlined area using microdissecting scissors. The wound area was sealed with Tegaderm dressing (Nexcare; catalog no. 55379) to prevent infection. Wound area was measured every day and calculated with ImageJ software. Average time to wound closure was monitored and considered complete when a scar was formed without any visible scab left.

Adoptive cell transfer. Tumor-free mice (C57BL/6 and BALB/c) and CT26 tumor-bearing mice were vaccinated 3 times; mice were sacrificed 1 week after the last vaccination, and splenocytes were used to magnetically isolate the lymphocyte population ($CD3^+$ T cells) (Miltenyl Biotec). Serum was also collected from vaccinated mice by intracardiac bleeding. Isolated lymphocytes and serum were injected in TC1 or CT26 tumor-bearing mice (challenged the day before adoptive transfer) that were sublethally irradiated (4–5 Gy) 3 days before adoptive transfer (i.v. and i.p., respectively). Serum was administered twice weekly for a total of 6 injections to another group of tumor-bearing mice.

Statistics. 2-tailed Student's *t* test was used to compare data sets where indicated. Single-step multiple-comparison Tukey test was performed for repeated measurements (Figure 3) at different time points. For $CD3^+$ T cell quantification in tumor sections (Figure 3, B and C), statistical analysis for the indicated comparisons was performed using Student's *t* test. Correlation between immune response by Tem1-TT treatment and tumor volume was analyzed with Pearson's rank correlation test (Figure 5), in which negative *r* was generated (inverse correlation); when *P* values are below 0.050, one variable tends to decrease, while the other increases. All *P* values presented are 2-sided. The log-rank test was performed for the survival curves in Supplemental Figures 2 and 4. A *P* value less than 0.05 was considered significant.

Study approval. All animal studies were approved by the IACUC and University Laboratory Animal Resources at the University of Pennsylvania. Mice were treated in accordance with University of Pennsylvania guidelines.

Acknowledgments

This project was supported by the Basser Research Center for BRCA, the Alliance for Cancer Gene Therapy, the NIH Director's New Innovator Award (1DP2OD008514), and the Pennsylvania Department of Health (4100051725).

Received for publication October 25, 2012, and accepted in revised form January 16, 2014.

Address correspondence to: Andrea Facciabene, Ovarian Cancer Research Center, University of Pennsylvania School of Medicine, Philadelphia, Pennsylvania 19104, USA. Phone: 215.746.7071; Fax: 215.573.5408; E-mail: facciabe@mail.med.upenn.edu.

1. Chung AS, Lee J, Ferrara N. Targeting the tumour vasculature: insights from physiological angiogenesis. *Nat Rev Cancer*. 2010;10(7):505–514.
2. Folkman J. Tumor angiogenesis: therapeutic implications. *N Engl J Med*. 1971;285(21):1182–1186.
3. Carmeliet P, Jain RK. Angiogenesis in cancer and other diseases. *Nature*. 2000;407(6801):249–257.
4. St Croix B, et al. Genes expressed in human tumor endothelium. *Science*. 2000;289(5482):1197–1202.
5. Jain RK. Molecular regulation of vessel maturation. *Nat Med*. 2003;9(6):685–693.
6. Teicher BA. Newer vascular targets: endosialin (review). *Int J Oncol*. 2007;30(2):305–312.
7. Buckanovich RJ, et al. Tumor vascular proteins as biomarkers in ovarian cancer. *J Clin Oncol*. 2007; 25(7):852–861.
8. Sasaroli D, et al. Novel surface targets and serum biomarkers from the ovarian cancer vasculature. *Cancer Biol Ther*. 2011;12(3):169–180.
9. Khong HT, Restifo NP. Natural selection of tumor variants in the generation of "tumor escape" phenotypes. *Nat Immunol*. 2002;3(11):999–1005.
10. Liu MA. DNA vaccines: an historical perspective and view to the future. *Immunol Rev*. 2010; 239(1):62–84.
11. Rice J, Ottensmeier CH, Stevenson FK. DNA vaccines: precision tools for activating effective immunity against cancer. *Nat Rev Cancer*. 2008;8(2):108–120.
12. Stevenson FK, Mander A, Chudley L, Ottensmeier CH. DNA fusion vaccines enter the clinic. *Cancer*

Immunol Immunother. 2011;60(8):1147–1151.
13. Facciabene A, et al. DNA and adenoviral vectors encoding carcinoembryonic antigen fused to immunoenhancing sequences augment antigen-specific immune response and confer tumor protection. *Hum Gene Ther*. 2006;17(1):81–92.
14. Brady J, Neal J, Sadakar N, Gasque P. Human endosialin (tumor endothelial marker 1) is abundantly expressed in highly malignant and invasive brain tumors. *J Neuropathol Exp Neurol*. 2004; 63(12):1274–1283.
15. Rouleau C, et al. Endosialin protein expression and therapeutic target potential in human solid tumors: sarcoma versus carcinoma. *Clin Cancer Res*. 2008; 14(22):7223–7236.
16. Carson-Walter EB, et al. Characterization of TEM1/endosialin in human and murine brain tumors. *BMC Cancer*. 2009;9:417.
17. Bagley RG. Endosialin: from vascular target to biomarker for human sarcomas. *Biomark Med*. 2009; 3(5):589–604.
18. MacFadyen J, Savage K, Wienke D, Isacke CM. Endosialin is expressed on stromal fibroblasts and CNS pericytes in mouse embryos and is downregulated during development. *Gene Expr Patterns*. 2007; 7(3):363–369.
19. MacFadyen JR, et al. Endosialin (TEM1, CD248) is a marker of stromal fibroblasts and is not selectively expressed on tumour endothelium. *FEBS Lett*. 2005;579(12):2569–2575.
20. Christian S, et al. Endosialin (Tem1) is a marker of tumor-associated myofibroblasts and tumor vessel-associated mural cells. *Am J Pathol*. 2008; 172(2):486–494.
21. Ohradanova A, et al. Hypoxia upregulates expression of human endosialin gene via hypoxia-inducible factor 2. *Br J Cancer*. 2008;99(8):1348–1356.
22. Rupp C, et al. Mouse endosialin, a C-type lectin-like cell surface receptor: expression during embryonic development and induction in experimental cancer neoangiogenesis. *Cancer Immun*. 2006;6:10.
23. Draenert R, et al. Comparison of overlapping peptide sets for detection of antiviral CD8 and CD4 T cell responses. *J Immunol Methods*. 2003;275(1–2):19–29.
24. Zhao A, Nunez-Cruz S, Li C, Coukos G, Siegel DL, Scholler N. Rapid isolation of high-affinity human antibodies against the tumor vascular marker Endosialin/TEM1, using a paired yeast-display/secretory scFv library platform. *J Immunol Methods*. 2011;363(2):221–232.
25. Kano MR, et al. Comparison of the effects of the kinase inhibitors imatinib, sorafenib, and transforming growth factor-beta receptor inhibitor on extravasation of nanoparticles from neovasculature. *Cancer Sci*. 2009;100(1):173–180.
26. Wood AK, Bunte RM, Cohen JD, Tsai JH, Lee WM, Sehgal CM. The antivascular action of physiotherapy ultrasound on a murine tumor: role of a microbubble contrast agent. *Ultrasound Med Biol*. 2007; 33(12):1901–1910.
27. Seiler GS, Ziemer LS, Schultz S, Lee WM, Sehgal CM. Dose-response relationship of ultrasound contrast agent in an in vivo murine melanoma model. *Cancer Imaging*. 2007;7:216–223.
28. van der Most RG, Currie A, Robinson BW, Lake RA. Cranking the immunologic engine with chemotherapy: using context to drive tumor antigen cross-presentation towards useful antitumor immunity. *Cancer Res*. 2006;66(2):601–604.
29. Ribas A, Timmerman JM, Butterfield LH, Economou JS. Determinant spreading and tumor responses after peptide-based cancer immunotherapy. *Trends Immunol*. 2003;24(2):58–61.
30. Seavey MM, Paterson Y. Anti-angiogenesis immunotherapy induces epitope spreading to Her-2/neu resulting in breast tumor immunoediting. *Breast Cancer (London)*. 2009;1:19–30.
31. Zhao X, et al. Vaccines targeting tumor blood vessel antigens promote CD8(+) T cell-dependent tumor eradication or dormancy in HLA-A2 transgenic mice. *J Immunol*. 2012;188(4):1782–1788.
32. Huang AY, et al. The immunodominant major histocompatibility complex class I-restricted antigen of a murine colon tumor derives from an endogenous retroviral gene product. *Proc Natl Acad Sci U S A*. 1996;93(18):9730–9735.
33. Rice J, Buchan S, Stevenson FK. Critical components of a DNA fusion vaccine able to induce protective cytotoxic T cells against a single epitope of a tumor antigen. *J Immunol*. 2002;169(7):3908–3913.
34. Feltkamp MC, et al. Vaccination with cytotoxic T lymphocyte epitope-containing peptide protects against a tumor induced by human papillomavirus type 16-transformed cells. *Eur J Immunol*. 1993; 23(9):2242–2249.
35. Singer AJ, Clark RA. Cutaneous wound healing. *N Engl J Med*. 1999;341(10):738–746.
36. Scappaticci FA, et al. Surgical wound healing complications in metastatic colorectal cancer patients treated with bevacizumab. *J Surg Oncol*. 2005; 91(3):173–180.
37. Sharma K, Marcus JR. Bevacizumab and wound-healing complications: mechanisms of action, clinical evidence, and management recommendations for the plastic surgeon. *Ann Plast Surg*. 2013; 71(4):434–440.
38. Ferrara N, et al. Vascular endothelial growth factor is essential for corpus luteum angiogenesis. *Nat Med*. 1998;4(3):336–340.
39. Fraser HM, Wulff C. Angiogenesis in the corpus luteum. *Reprod Biol Endocrinol*. 2003;1:88.
40. Demir R, Kayisli UA, Cayli S, Huppertz B. Sequential steps during vasculogenesis and angiogenesis in the very early human placenta. *Placenta*. 2006; 27(6–7):535–539.
41. Klauber N, Rohan RM, Flynn E, D'Amato RJ. Critical components of the female reproductive pathway are suppressed by the angiogenesis inhibitor AGM-1470. *Nat Med*. 1997;3(4):443–446.
42. Rutland CS, Mukhopadhyay M, Underwood S, Clyde N, Mayhew TM, Mitchell CA. Induction of intrauterine growth restriction by reducing placental vascular growth with the angioinhibin TNP-470. *Biol Reprod*. 2005;73(6):1164–1173.
43. Ito T, Ando H, Handa H. Teratogenic effects of thalidomide: molecular mechanisms. *Cell Mol Life Sci*. 2011;68(9):1569–1579.
44. Lax S, et al. CD248/Endosialin is dynamically expressed on a subset of stromal cells during lymphoid tissue development, splenic remodeling and repair. *FEBS Lett*. 2007;581(18):3550–3556.
45. Huang HP, et al. Gene targeting and expression analysis of mouse Tem1/endosialin using a lacZ reporter. *Gene Expr Patterns*. 2011;11(5–6):316–326.
46. Kamat BR, Brown LF, Manseau EJ, Senger DR, Dvorak HF. Expression of vascular permeability factor/vascular endothelial growth factor by human granulosa and theca lutein cells. Role in corpus luteum development. *Am J Pathol*. 1995; 146(1):157–165.
47. Delli Carpini J, Karam AK, Montgomery L. Vascular endothelial growth factor and its relationship to the prognosis and treatment of breast, ovarian, and cervical cancer. *Angiogenesis*. 2010;13(1):43–58.
48. Rafii S. Vaccination against tumor neovascularization: Promise and reality. *Cancer Cell*. 2002; 2(6):429–431.
49. Wei YQ, et al. Immunotherapy of tumors with xenogeneic endothelial cells as a vaccine. *Nat Med*. 2000; 6(10):1160–1166.
50. Okaji Y, et al. Vaccination with autologous endothelium inhibits angiogenesis and metastasis of colon cancer through autoimmunity. *Cancer Sci*. 2004; 95(1):85–90.
51. Zhao X, et al. Intratumoral IL-12 gene therapy results in the crosspriming of Tc1 cells reactive against tumor-associated stromal antigens. *Mol Ther*. 2011;19(4):805–814.
52. Chinnasamy D, et al. Gene therapy using genetically modified lymphocytes targeting VEGFR-2 inhibits the growth of vascularized syngenic tumors in mice. *J Clin Invest*. 2010;120(11):3953–3968.
53. Bagley RG, et al. Human endothelial precursor cells express tumor endothelial marker 1/endosialin/CD248. *Mol Cancer Ther*. 2008;7(8):2536–2546.
54. Simonavicius N, Robertson D, Bax DA, Jones C, Huijbers IJ, Isacke CM. Endosialin (CD248) is a marker of tumor-associated pericytes in high-grade glioma. *Mod Pathol*. 2008;21(3):308–315.
55. Wesseling P, Schlingemann RO, Rietveld FJ, Link M, Burger PC, Ruiter DJ. Early and extensive contribution of pericytes/vascular smooth muscle cells to microvascular proliferation in glioblastoma multiforme: an immuno-light and immuno-electron microscopic study. *J Neuropathol Exp Neurol*. 1995; 54(3):304–310.
56. Carson-Walter EB, Watkins DN, Nanda A, Vogelstein B, Kinzler KW, St Croix B. Cell surface tumor endothelial markers are conserved in mice and humans. *Cancer Res*. 2001;61(18):6649–6655.
57. Christian S, et al. Molecular cloning and characterization of endosialin, a C-type lectin-like cell surface receptor of tumor endothelium. *J Biol Chem*. 2001; 276(10):7408–7414.
58. Rettig WJ, Garin-Chesa P, Healey JH, Su SL, Jaffe EA, Old LJ. Identification of endosialin, a cell surface glycoprotein of vascular endothelial cells in human cancer. *Proc Natl Acad Sci U S A*. 1992; 89(22):10832–10836.
59. Buckanovich RJ, et al. Use of immuno-LCM to identify the in situ expression profile of cellular constituents of the tumor microenvironment. *Cancer Biol Ther*. 2006;5(6):635–642.
60. Walter-Yohrling J, et al. Murine endothelial cell lines as models of tumor endothelial cells. *Clin Cancer Res*. 2004;10(6):2179–2189.
61. Davies G, Cunnick GH, Mansel RE, Mason MD, Jiang WG. Levels of expression of endothelial markers specific to tumour-associated endothelial cells and their correlation with prognosis in patients with breast cancer. *Clin Exp Metastasis*. 2004; 21(1):31–37.
62. Becker R, et al. Tumor stroma marker endosialin (Tem1) is a binding partner of metastasis-related protein Mac-2 BP/90K. *FASEB J*. 2008; 22(8):3059–3067.
63. Tomkowicz B, et al. Interaction of endosialin/TEM1 with extracellular matrix proteins mediates cell adhesion and migration. *Proc Natl Acad Sci U S A*. 2007;104(46):17965–17970.
64. Nanda A, et al. Tumor endothelial marker 1 (Tem1) functions in the growth and progression of abdominal tumors. *Proc Natl Acad Sci U S A*. 2006; 103(9):3351–3356.
65. Sparwasser T, et al. Bacterial DNA and immunostimulatory CpG oligonucleotides trigger maturation and activation of murine dendritic cells. *Eur J Immunol*. 1998;28(6):2045–2054.
66. Panina-Bordignon P, Tan A, Termijtelen A, Demotz S, Corradin G, Lanzavecchia A. Universally immunogenic T cell epitopes: promiscuous binding to human MHC class II and promiscuous recognition by T cells. *Eur J Immunol*. 1989;19(12):2237–2242.
67. Rice J, Elliott T, Buchan S, Stevenson FK. DNA fusion vaccine designed to induce cytotoxic T cell responses against defined peptide motifs: implications for cancer vaccines. *J Immunol*. 2001; 167(3):1558–1565.
68. Buchan S, Gronevik E, Mathiesen I, King CA, Stevenson FK, Rice J. Electroporation as a "prime/boost" strategy for naked DNA vaccination against a tumor antigen. *J Immunol*. 2005; 174(10):6292–6298.
69. Ahlen G, et al. In vivo electroporation enhances the

immunogenicity of hepatitis C virus nonstructural 3/4A DNA by increased local DNA uptake, protein expression, inflammation, and infiltration of CD3+ T cells. *J Immunol*. 2007;179(7):4741–4753.
70. Stevenson FK, Rice J, Ottensmeier CH, Thirdborough SM, Zhu D. DNA fusion gene vaccines against cancer: from the laboratory to the clinic. *Immunol Rev*. 2004;199:156–180.
71. Stevenson FK, Ottensmeier CH, Rice J. DNA vaccines against cancer come of age. *Curr Opin Immunol*. 2010;22(2):264–270.
72. Chen CH, et al. Enhancement of DNA vaccine potency by linkage of antigen gene to an HSP70 gene. *Cancer Res*. 2000;60(4):1035–1042.
73. Yewdell JW, Bennink JR. Immunodominance in major histocompatibility complex class I-restricted T lymphocyte responses. *Annu Rev Immunol*. 1999; 17:51–88.
74. Oosterhuis K, et al. Preclinical development of highly effective and safe DNA vaccines directed against HPV 16 E6 and E7. *Int J Cancer*. 2011; 129(2):397–406.
75. Seavey MM, Maciag PC, Al-Rawi N, Sewell D, Patterson Y. An anti-vascular endothelial growth factor receptor 2/fetal liver kinase-1 Listeria monocytogenes anti-angiogenesis cancer vaccine for the treatment of primary and metastatic Her-2/neu+ breast tumors in a mouse model. *J Immunol*. 2009; 182(9):5537–5546.
76. van den Heuvel MJ, et al. A review of trafficking and activation of uterine natural killer cells. *Am J Reprod Immunol*. 2005;54(6):322–331.
77. Bilinski MJ, et al. Uterine NK cells in murine pregnancy. *Reprod Biomed Online*. 2008;16(2):218–226.
78. Schafer M, Werner S. Cancer as an overhealing wound: an old hypothesis revisited. *Nat Rev Mol Cell Biol*. 2008;9(8):628–638.
79. Facciabene A, et al. Vectors encoding carcinoembryonic antigen fused to the B subunit of heat-labile enterotoxin elicit antigen-specific immune responses and antitumor effects. *Vaccine*. 2007; 26(1):47–58.
80. Raj A, van den Bogaard P, Rifkin SA, van Oudenaarden A, Tyagi S. Imaging individual mRNA molecules using multiple singly labeled probes. *Nat Methods*. 2008;5(10):877–879.
81. Mennuni C, et al. Efficient induction of T-cell responses to carcinoembryonic antigen by a heterologous prime-boost regimen using DNA and adenovirus vectors carrying a codon usage optimized cDNA. *Int J Cancer*. 2005;117(3):444–455.
82. Sehgal CM, et al. Renal blood flow changes induced with endothelin-1 and fenoldopam mesylate at quantitative Doppler US: initial results in a canine study. *Radiology*. 2001;219(2):419–426.
83. Sehgal CM, Arger PH, Rowling SE, Conant EF, Reynolds C, Patton JA. Quantitative vascularity of breast masses by Doppler imaging: regional variations and diagnostic implications. *J Ultrasound Med*. 2000;19(7):427–440.
84. Cha HR, et al. Mucosa-associated epithelial chemokine/CCL28 expression in the uterus attracts CCR10+ IgA plasma cells following mucosal vaccination via estrogen control. *J Immunol*. 2011; 187(6):3044–3052.
85. Li Y, et al. Active immunization against the vascular endothelial growth factor receptor flk1 inhibits tumor angiogenesis and metastasis. *J Exp Med*. 2002; 195(12):1575–1584.